ELSEVIER

Microelectronics Journal 37 (2006) 1471–1476

Microelectronics Journal

www.elsevier.com/locate/mejo

Reading the footprints of strained islands

A. Rastelli[a,*], M. Stoffel[a], G. Katsaros[a], J. Tersoff[b], U. Denker[a], T. Merdzhanova[a], G.S. Kar[a], G. Costantini[a], K. Kern[a], H. von Känel[c,d], O.G. Schmidt[a]

[a]*Max-Planck-Institut für Festkörperforschung, Heisenbergstrasse 1, D-70569 Stuttgart, Germany*
[b]*IBM Research Division, T. J. Watson Research Center, Yorktown Heights, NY 10598, USA*
[c]*ETH Zürich, Laboratorium für Festkörperphysik, CH-8093 Zürich, Switzerland*
[d]*INFM and L-NESS, Dipartimento di Fisica, Politecnico di Milano, Via Anzani 52, I-22100 Como, Italy*

Received 18 May 2006
Available online 17 July 2006

Abstract

We report on recent advances in the understanding of surface processes occurring during growth and post-growth annealing of strained islands which may find application as self-assembled quantum dots. We investigate the model system SiGe/Si(0 0 1) by a new approach based on "reading the footprints" which islands leave on the substrate during their growth and evolution. Such footprints consist of trenches carved in the Si substrate. We distinguish between surface footprints and footprints buried below the islands. The former allow us to discriminate islands which are in the process of growing from those which are shrinking. Islands with steep morphologies grow at the expense of smaller and shallower islands, consistent with the kinetics of anomalous coarsening. While shrinking, islands change their shape according to thermodynamic predictions. Buried footprints are investigated by removing the SiGe epilayer by means of selective wet chemical etching. Their reading shows that: (i) during post-growth annealing islands move laterally because of surface-mediated Si–Ge intermixing; (ii) a tree-ring structure of trenches is created by dislocated islands during their "cyclic" growth. This allows us to distinguish coherent from dislocated islands and to establish whether the latter are the result of island coalescence.

Keywords: Self-assembled quantum dots; Ge/Si; Selective etching; Morphological transitions

1. Introduction

The most elegant and convenient method to fabricate nanometer-scale objects is to exploit the capability of certain material systems to self-assemble nano-structures. For instance, defect-free semiconductor "quantum dots" can be created by means of lattice-mismatched hetero-epitaxial growth. In the Stranski–Krastanow growth mode, the elastic strain stored in the growing film is relaxed by the formation of three-dimensional (3D) islands on top of a thin, pseudomorphic wetting layer. Among the different material combinations, the SiGe/Si(0 0 1) system can be considered as a model playground for understanding the physics of self-assembled island growth.

At typical growth temperatures (550–850 °C), islands first appear as shallow unfaceted "prepyramids" (PP) [1–3]. With increasing size they undergo a shape transition to truncated, partially faceted pyramids (TP), which then evolve into fully {1 0 5} faceted pyramids (P) [1–5]. At a critical size, pyramids undergo a transition to multifaceted islands bounded by steeper facets, referred to as "domes" (D) [4–6]. If enough Si is present in the epilayer, either provided by the flux or by the Si substrate via surface diffusion, the morphological evolution continues by introduction of facets with increasing slope [7,8]. This sequence is summarized in Fig. 1, where scanning probe microscopy topographs of representative islands are shown in 3D view. Figs. 1(a)–(c) illustrate the PP-to-P evolution. Pyramids transform into domes [Fig. 1(e)] via intermediate, metastable shapes [TD, Fig. 1(d)] [6,9] and then into "barns" [B, Fig. 1(f)]. The evolution of coherent shapes is characterized by a monotonic increase of aspect ratio achieved by the introduction of increasingly steep orientation close to the island base and a consequent lifting of the shallow orientations towards the island apex.

*Corresponding author. Tel.: +49 711 689 1231; fax: +49 711 689 1010.
E-mail address: A.Rastelli@fkf.mpg.de (A. Rastelli).

0026-2692/$ - see front matter © 2006 Elsevier Ltd. All rights reserved.
doi:10.1016/j.mejo.2006.05.029

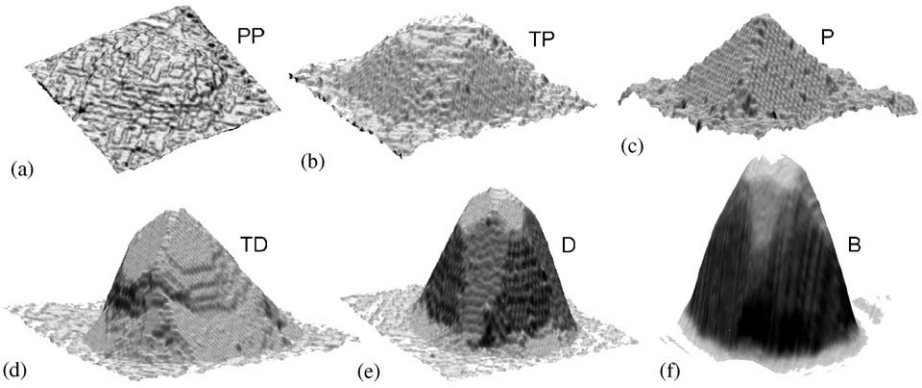

Fig. 1. Scanning tunneling microscopy (a)–(e) and AFM (f) images of representative islands illustrating the morphological evolution of coherent SiGe islands on Si(0 0 1). Islands are prepyramids [PP, (a)], truncated pyramids [TP, (b)], pyramids [P, (c)], islands with shape intermediate between pyramids and domes [TD, (d)], domes [D, (e)], barns [B, (f)]. Images were obtained on several samples grown under different conditions. For details, see Refs. [18,8].

By reducing the Ge fraction x in the islands, and hence the lattice mismatch, the volumes at which the shape transitions occur increase approximately with x^{-6} [4,10]. Other phenomena, such as Si–Ge intermixing [11–14], modification of the wetting layer surface reconstruction [15], formation of *trenches* at the island perimeter [13,16,17] and eventually dislocation introduction (in this case islands are referred to as "superdomes" [11]) provide additional strain-relaxation mechanisms.

Many different microscopic techniques have been used to characterize self-assembled islands, both during growth [6,19] and at room temperature (RT) after growth [1,3–5,7,20]. The former approach allows the direct imaging of the growth dynamics, but is usually technologically challenging or is limited in resolution or accessible growth conditions. The latter only provides "snapshots" of the surface "frozen" at RT.

In this paper, we report on the observation and interpretation of *footprints* left by SiGe islands on the substrate surface. Such footprints, which we study by RT scanning probe microscopy, consist of trenches forming at the island perimeter when the growth is performed at sufficiently high temperatures [21,16]. Analogous to fossile footprints, a careful reading of such tracks allows us to gather information on different phenomena occurring during growth. We distinguish between footprints on the surface (see Section 3) and footprints buried below the SiGe islands (see Section 4). The latter are observed by selectively removing the SiGe material by wet chemical etching. The most unexpected result of this analysis is that islands move laterally on the surface during post-growth annealing. We interpret this phenomenon as a mechanism for alloying, and hence strain relaxation, exclusively via surface diffusion.

2. Experimental methods

The samples studied here were grown by solid-source molecular beam epitaxy (MBE). After deoxidation and Si-buffer growth, Ge was deposited at a rate of 0.04 monolayers/s (ML/s) at a substrate temperature T_s between 620 and 840 °C. The samples were cooled to RT before characterization. In order to study buried footprints, some specimens were etched with a mixture of HF:1 H_2O_2: 2 CH_3COOH: 3 (BPA solution), which is known to etch selectively SiGe alloys over pure Si [22]. Qualitative information on the island composition profiles are obtained by using a different etchant, namely NH_4OH: H_2O_2 [23]. The selectivity of BPA is 1100:1 for $Si_{0.6}Ge_{0.4}$ over Si (NH_4OH: H_2O_2 does not etch pure Si). The etching rate at RT for a $Si_{0.6}Ge_{0.4}$ alloy is about 110 nm/s for BPA and 0.007 nm/s for NH_4OH: H_2O_2. The samples were characterized by ex situ atomic force microscopy (AFM) in tapping mode. The *same* surface areas were imaged prior to and after etching, providing unambiguous information on the island evolution and composition profiles.

3. Footprints on the surface: kinetic evolution and equilibrium morphology of SiGe islands

Fig. 2(a) shows an AFM image of a sample obtained after deposition of six monolayers (ML) of Ge on Si(0 0 1) at $T_s = 840$ °C. The color scale according to the local surface slope with respect to the (0 0 1) plane allows steep and shallow facets to be distinguished. We observe different island morphologies, such as domes (D), TDs, pyramids (P), TPs and unfaceted prepyramids (PP, not shown in Fig. 2(a)). The plot of the aspect ratio r vs. volume [Fig. 2(b)] indicates that different island sizes correspond to different shapes. (Here r is defined as the ratio between height and square root of the base area.)

The information contained in Figs. 2(a) and (b) alone is not sufficient to establish how each island was evolving before the sample was cooled to RT. In particular, we do not know whether the small TPs were in the process of growing and transforming to pyramids or shrinking and disappearing. An answer to this question is provided by Fig. 2(c), in which the color scale enhances the corrugations of the wetting layer. We observe trenches (dark in the figure) surrounding each island, but also "empty" trenches

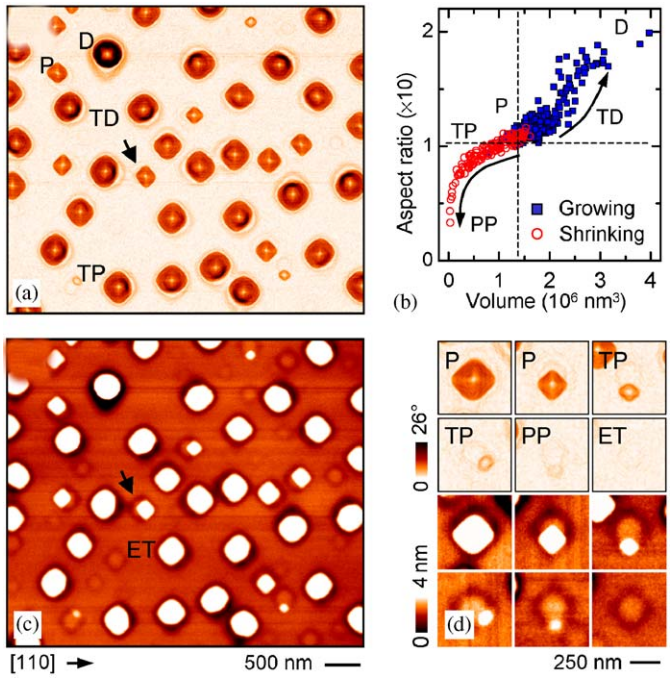

Fig. 2. AFM image of SiGe islands obtained by deposition of 6 ML Ge on Si(0 0 1) at 840 °C with color scale according to surface slope (a) and height (c). Statistical analysis of island shape versus volume (b). In (c), empty trenches (ET), which can be interpreted as footprints left by dissolved islands, are also seen. Sequence of AFM magnifications illustrating shrinking pyramids and the pyramid-to-prepyramid transition (d).

(ET), which do not surround any island. The latter are footprints left by islands which formed, grew, then shrunk and disappeared before the measurement was performed. In Fig. 2(c) we can also identify shrinking islands, such as that pointed at by an arrow in Figs. 2(a) and (c), whose base area is smaller than the trench area. Their relative position with respect to the trench center suggests that part of the material initially composing the shrinking islands has migrated towards the larger nearby TDs or Ds [24]. This observation is consistent with a coarsening process, in which islands larger than a certain size grow at the expense of islands with smaller sizes [6,11,25]. By distinguishing shrinking from growing islands in Fig. 2(b) and by performing a careful analysis of the island facets [24], we find that the critical size separating shrinking and growing islands corresponds to the P–TD transition, i.e. that TDs and Ds grow at the expense of smaller PPs, TPs and Ps. This corresponds exactly to the proposed anomalous coarsening process [26], because the P–TD transition is a first-order transition marked by a discontinuous change in island chemical potential with volume [27,28].

A closer inspection of islands at different stages of the shrinking process [Fig. 1(d)] leads us to draw another important conclusion: islands change their shape while shrinking and undergo a reverse morphological transition from P to TP and eventually to PP, as a result of their volume decrease. Similar conclusions were previously drawn in Ref. [3] based on the observation of TPs together with larger TDs. However, no direct proof of the shrinking nature of small TPs was provided in Ref. [3]. We can thus conclude that while the evolution of the island ensemble follows the kinetics of ripening, the morphology of each island is mainly determined by thermodynamics [28,2,3].

4. Buried footprints

The above discussion demonstrates that, due to the trenches, the RT scanning probe microscopy data provide much more information than simple snapshots of the surface morphology. Since the Si–Ge island material is more mobile than the trenches carved into the Si substrate, we can aim to reveal trenches buried below the islands by selectively etching the SiGe alloy [16]. This simple method enables us to gather new insights into the intermixing-induced dome-to-pyramid transition occurring during post-growth annealing [12,29] and in the evolution of dislocated superdomes [11,30].

4.1. Lateral island motion during post-growth annealing

Fig. 3(a) shows the surface of a sample obtained upon deposition of 10 ML of Ge on Si(0 0 1) at $T_s = 740\,^{\circ}C$. A detailed analysis shows that the islands have an average height of 41 ± 4 nm and consist of a monomodal distribution of barns [7,8].

As reported previously, post-growth annealing causes island coarsening and strong Si–Ge intermixing [6,11,12,21], leading to a reverse transition of domes to pyramids through intermediate shapes. However, the mechanism through which alloying is achieved has not been clarified yet. Fig. 3(b) shows an AFM image of a sample obtained after deposition of 10 ML of Ge and subsequent annealing at $T_s = 740\,^{\circ}C$ for 20 min. During annealing, the barns transform back to TDs and pyramids. AFM scans taken after selective etching in BPA solution are shown in Figs. 3(c)–(d) for the samples displayed in Figs. 3(a)–(b). Prior to annealing [Fig. 3(c)], circular Si plateaux remain, which are surrounded by an approximately square trench with sides parallel to the [1 0 0] and [0 1 0] directions [16]. The etching of the annealed samples reveals that the original Si-plateaux, or portions of them, are still present buried under the islands [see Fig. 3(d)]. While prior to annealing the Si-plateaux are close to the island centers, after annealing they are at the island edge. We can thus conclude that during annealing islands do not only intermix and change their shape, but also *move* laterally on the surface. This is better seen in Figs. 3(e)–(f), where linescans of the representative islands marked in Figs. 3(a)–(b) are plotted before and after etching in BPA solution.

With reference to Figs. 3(e)–(f), we can qualitatively describe the island motion as due to material removal from the left side of the island and deposition on the right side. As a consequence of the motion, a part of the initially circular Si-plateau becomes uncapped and the Si atoms

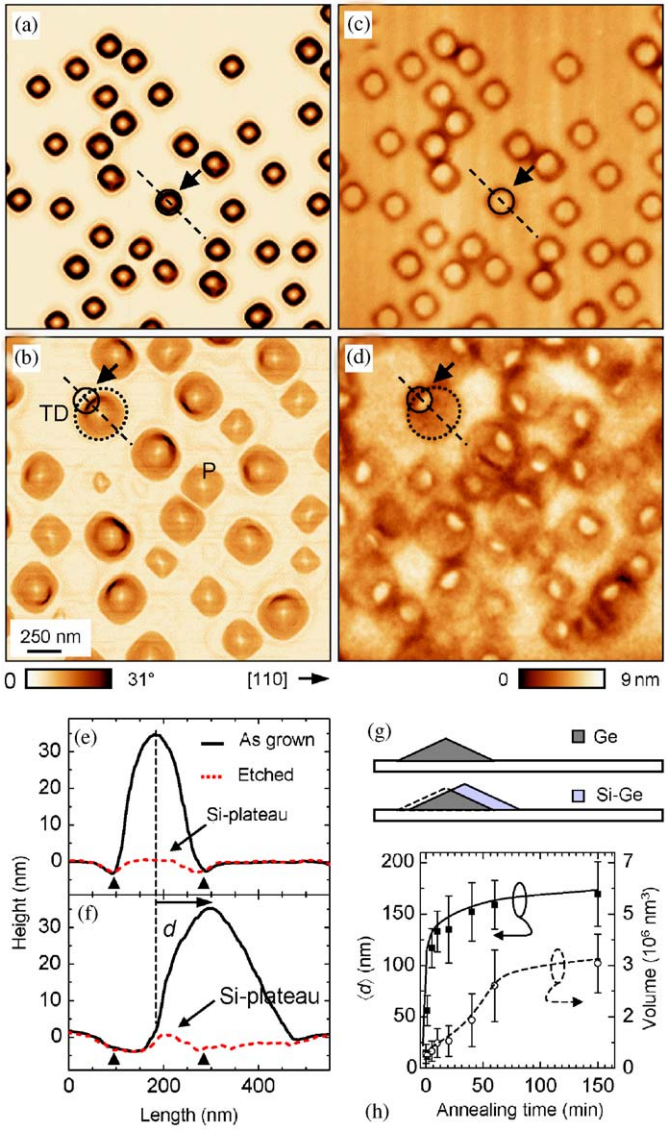

Fig. 3. Representative AFM images of SiGe islands before (a), (b) and after selective etching in BPA solution (c), (d) of samples with 10 ML Ge grown at 740 °C. In (a), (c) the sample was cooled to RT immediately after growth while in (b), (d) the sample was annealed for 20 min at 740 °C. Circles pointed at by arrows in (c), (d) indicate representative Si-plateaux. Linescans of two representative SiGe islands before (e) and after annealing (f). Triangles mark the position of the Si-plateau edges before annealing. The arrow in (f) represents the displacement d undergone by the island center during annealing. (g) Schematic illustration of island motion. (h) Average displacement and volume of islands as a function of annealing time.

composing it migrate away from the compressed region at the foot of the new island left edge. In contrast, the remaining part of the Si-plateau buried under the island is preserved because its modification would require the contribution of bulk interdiffusion. At the same time, the right island edge advances gradually generating a new, shallower trench at its foot [visible as a dark area in Fig. 3(d)]. The Si removed from the island perimeter is probably added onto the growing front of the island

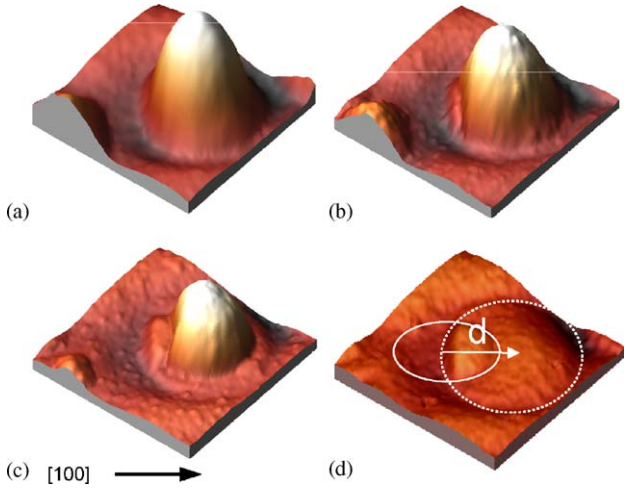

Fig. 4. AFM images (440 × 440 nm^2) of a SiGe island annealed for 10 min at 740 °C (a) and etched in $NH_4OH:H_2O_2$ at RT for 80 min (b), 170 min (c) and 620 min (d).

together with material of the original island, leading to an *efficient Si–Ge intermixing* achieved exclusively by surface diffusion. Therefore, the island volume increases and the average Ge fraction x of the material composing the island decreases. As a result of strain release [12,10], domes and barns become unstable and their shape changes to TD or pyramid. From Fig. 3(f), we also note that the left side of the TD island, which we interpret as a remainder of the island before annealing, is still dome-like, consistently with a Ge-rich composition while the right side is pyramid-like because of the Si added during the motion.

A direct proof of the asymmetric composition of the annealed islands is provided by subsequent etching experiments performed by $NH_4OH:H_2O_2$ [23] (Fig. 4). By imaging the same area after each etching step we see that the left side of the island shown in Fig. 4(a) is etched faster than the right side [Figs. 4(b)–(c)], consistent with a Ge-richer composition of the left side. Since the left side sits on top of the half-moon shaped plateau [Fig. 4(d)] we interpret this side as a remainder of the original island before annealing. The right island side is Si-richer because of the Si added to this side during the motion.

The origin of the island motion can be understood with a simple thermodynamic model for a strictly faceted pyramidal island of pure Ge, as shown schematically in cross-section in the top panel of Fig. 3(g). By assuming an initial small motion [bottom panel of Fig. 3(g)] it is possible to show that the motion is self-sustaining and proceeds until most of the original island has intermixed with Si from the substrate [31]. From the AFM images taken after selective etching we determine the displacement d of an island as the distance between the position of the island center prior to and after annealing [see small and large circles in Figs. 3(d) and 4(d)]. The average displacement is shown in Fig. 3(h) as a function of annealing time and indicates that the motion is initially fast and then slows down as expected.

Meanwhile, the average island volume [Fig. 3(h)] also increases as a result of Si incorporation and, possibly, island ripening.

A final question concerns the conditions required to initiate self-sustaining lateral motion and mixing. For islands very close to each other prior to annealing, we measure a strong correlation between the direction of motion and the direction away from the nearest neighbor, suggesting that an environmental asymmetry, such as a strain gradient, triggers the motion [32]. We also find that the *magnitude* of the motion is always comparable to the island radius, and shows no obvious correlation with environment, suggesting that the motion is self-sustaining, and the role of the environment acts only as an initial trigger. We note that the island motion during annealing can be suppressed if the island position is fixed by surface strain energy modulations caused by a buried island layer [32].

4.2. "Dendrochronology" of dislocated islands

Trench formation and intermixing are effective ways to release strain and to delay the introduction of dislocations. However, superdomes are unavoidably observed for large amounts of deposited Ge. In Fig. 5(a), we show an AFM image of a sample obtained after deposition of 15 ML of Ge at $T_s = 800\,^{\circ}C$. The island at the center of the image is a superdome whose surface has been characterized in detail in Ref. [33].

The selective etching of this sample in BPA solution reveals that superdomes leave over a complex "tree-ring" or staircase structure [see Fig. 5(b)]. Line scans of the superdome prior to and after etching are shown in Fig. 5(c). The bottommost curve represents the second derivative (in arbitrary units) of the AFM topograph of the etched sample and allows a clear identification of the ring positions. At least seven rings, pointed at by arrows, can be identified. Following the arguments above we can use the rings to track the evolution of the superdome and its environment, analogous to the study of real tree-rings ("dendrochronology"). The rings are produced by a discontinuous expansion of the superdome perimeter and the formation of new, deeper trenches for every cycle [see Fig. 5(f)]. This phenomenon was observed in real-time in Ref. [30]. We can thus interpret the number of rings as the number of dislocations introduced in the island during its growth and easily distinguish coherent from dislocated islands.

With this method we measured how the critical volume for dislocation introduction increases [34] with increasing growth temperature because of Si–Ge intermixing [34,35]. Moreover, we find that some superdomes are the result of the coalescence of two or more islands [see Fig. 5(d)]. Island coalescence appears to be dominant at relatively low growth temperatures (less than about 700 °C). At higher temperatures, ripening is efficient and material can migrate from smaller islands to larger islands (see Section 3) before

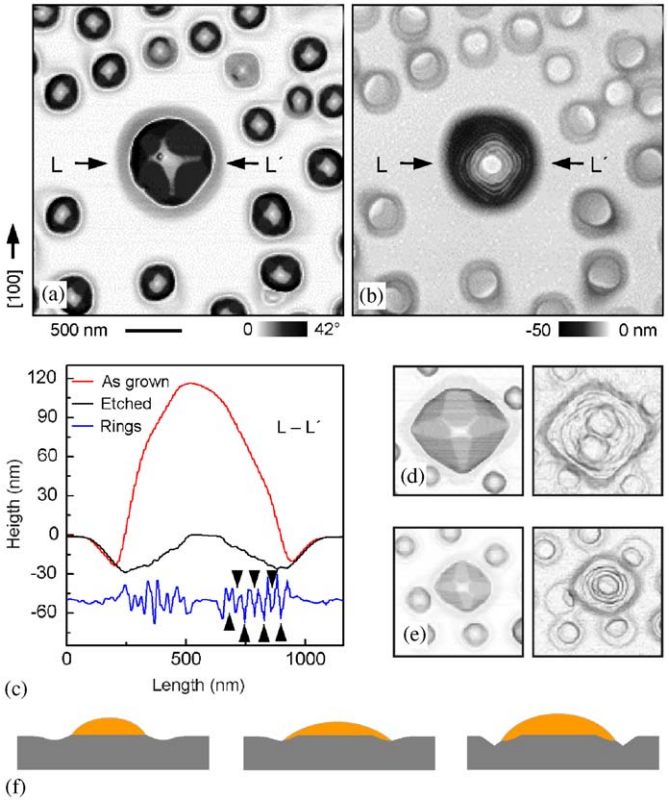

Fig. 5. AFM images of a SiGe superdome (15 ML Ge grown at 800 °C) prior to (a) and after etching in BPA solution (b). The colorscale of (b) is enhanced by a second derivative filtering. (c) Line scans (L–L′) of the AFM images along the [0 1 0] direction. The bottommost linescan represents the numerical second derivative of the topograph shown in (b), with triangles indicating the ring positions. AFM magnifications of (d) a superdome generated by the coalescence of two islands (15 ML Ge grown at 620 °C), (e) a superdome and an island moving away from it (15 ML Ge grown at 700 °C). (f) A schematic representation of the mechanism leading to the formation of the ring structure seen in (b).

the occurrence of coalescence. A competing mechanism is island motion produced by strain repulsion, as demonstrated by the presence of half-moon structures buried below islands close to superdomes [Fig. 5(e)]. This observation shows how the study of island footprints can give information on the evolution of dislocated islands and their environment.

5. Conclusions

In this paper, we have reported on the observation and interpretation of footprints left behind by strained islands. Different processes and phenomena occurring during the island evolution were unambiguously traced back by studying such footprints: (i) we followed the disappearance of small islands during anomalous coarsening and observed the reverse of a morphological transition predicted theoretically in Refs. [2,3]; (ii) upon post-growth annealing islands were observed to move laterally to achieve alloying exclusively through surface diffusion; (iii) a tree-ring

structure was discovered buried under dislocated islands, with each ring corresponding to a dislocation.

Acknowledgments

This work was supported by the BMBF (03N8711). We acknowledge K. von Klitzing for his continuous support and interest, S. Kiravittaya for fruitful discussions and E. Coric for assistance in the AFM measurements.

References

[1] A. Vailionis, et al., Phys. Rev. Lett. 85 (2000) 3672.
[2] J. Tersoff, B.J. Spencer, A. Rastelli, H. von Känel, Phys. Rev. Lett. 89 (2002) 196104.
[3] A. Rastelli, H. von Känel, B.J. Spencer, J. Tersoff, Phys. Rev. B 68 (2003) 115301.
[4] J.A. Floro, et al., Phys. Rev. Lett. 80 (1998) 4717.
[5] G. Medeiros-Ribeiro, et al., Science 279 (1998) 353.
[6] F.M. Ross, R.M. Tromp, M.C. Reuter, Science 286 (1999) 1931.
[7] E. Sutter, P. Sutter, J.E. Bernard, Appl. Phys. Lett. 84 (2004) 2262.
[8] M. Stoffel, A. Rastelli, T. Merdzhanova, O.G. Schmidt, Microelectr. J., in press, 10.1016/j.mejo.2006.05.025.
[9] F. Montalenti, et al., Phys. Rev. Lett. 93 (2004) 216102.
[10] A. Rastelli, M. Kummer, H. von Känel, Phys. Rev. Lett. 87 (2001) 256101.
[11] T.I. Kamins, G. Medeiros-Ribeiro, D.A.A. Ohlberg, R.S. Williams, J. Appl. Phys. 85 (1999) 1159.
[12] T.I. Kamins, G. Medeiros-Ribeiro, D.A.A. Ohlberg, R.S. Williams, Appl. Phys. A 67 (1998) 727.
[13] S.A. Chaparro, et al., Phys. Rev. Lett. 83 (1999) 1199.
[14] U. Denker, M. Stoffel, O.G. Schmidt, Phys. Rev. Lett. 90 (2003) 196102.
[15] U. Köhler, et al., Ultramicroscopy 42–44 (1992) 832.
[16] U. Denker, O.G. Schmidt, N.Y. Jin-Philipp, K. Eberl, Appl. Phys. Lett. 78 (2001) 3723.
[17] P. Sonnet, P.C. Kelires, Appl. Phys. Lett. 85 (2004) 203.
[18] A. Rastelli, H. von Känel, Surf. Sci. 532–535 (2003) 769.
[19] B. Voigtländer, Surf. Sci. Reports 43 (2001) 127.
[20] O.G. Schmidt, C. Lange, K. Eberl, Appl. Phys. Lett. 75 (1999) 1905.
[21] T.I. Kamins, E.C. Carr, R.S. Williams, S.J. Rosner, J. Appl. Phys. 81 (1997) 211.
[22] T.K. Carns, M.O. Tanner, K.L. Wang, J. Electrochem. Soc. 142 (1995) 1260.
[23] G. Katsaros, A. Rastelli, M. Stoffel, G. Isella, H. von Känel, A.M. Bittner, J. Tersoff, U. Denker, O.G. Schmidt, G. Costantini, K. Kern, Surf. Sci. 600 (2006) 2608.
[24] A. Rastelli, et al., Phys. Rev. Lett. 95 (2005) 026103.
[25] N. Vostokov, et al., Phys. Low-Dimensional Struct. 3/4 (2001) 295.
[26] F.M. Ross, J. Tersoff, R.M. Tromp, Phys. Rev. Lett. 80 (1998) 984.
[27] J. Tersoff, Appl. Phys. Lett. 83 (2003) 353.
[28] I. Daruka, J. Tersoff, A.L. Barabási, Phys. Rev. Lett. 82 (1999) 2753.
[29] W.L. Henstrom, et al., Appl. Phys. Lett. 77 (2000) 1623.
[30] F.K. Legoues, et al., Phys. Rev. Lett. 73 (1994) 300.
[31] U. Denker, et al., Phys. Rev. Lett. 94 (2005) 216203.
[32] M. Stoffel, A. Rastelli, S. Kiravittaya, O.G. Schmidt, Phys. Rev. B 72 (2005) 205411.
[33] A. Rastelli, H. von Känel, Surf. Sci. Lett. 515 (2002) L493.
[34] T. Merdzhanova, S. Kiravittaya, A. Rastelli, M. Stoffel, O.G. Schmidt, Phys. Rev. Lett. 96 (2006) 226103.
[35] M. De Seta, G. Capellini, F. Evangelisti, C. Spinella, J. Appl. Phys. 92 (2002) 614.